Proceedings of IPC'02
4th International Pipeline Conference
September 29-October 3, 2002, Calgary, Alberta, Canada

IPC2002-27169

A PRELIMINARY STRAIN-BASED DESIGN CRITERION FOR PIPELINE GIRTH WELDS

Yong-Yi Wang
Engineering Mechanics Corporation of Columbus
3518 Riverside Dr., Suite 202
Columbus, OH 43221, USA
wangemc2@columbus.rr.com

David Rudland
Engineering Mechanics Corporation of Columbus
3518 Riverside Dr., Suite 202
Columbus, OH 43221, USA
rudland_emc2@columbus.rr.com

Rudi Denys
University of Gent
St. Pietersnieuwstraat 41
B-9000, Gent, Belgium
rudi.denys@rug.ac.be

David Horsley
TransCanada Pipelines Limited
450 1st Street SW
Calgary, Alberta T2P 5H1, Canada
david_horsley@transcanada.com

ABSTRACT

The strain capacity of girth welds containing surface-breaking welding defects is examined through numerical analysis and experimental verification under a PRCI (Pipeline Research Council International) funded project. Some important insights on the various factors affecting the girth weld strain capacity are generated. The defect size is identified as one of the most important factors in determining strain capacity of a girth weld. Other factors, such as the strain hardening rate of the pipe and weld metals, weld strength mismatch, fracture toughness, and weld cap height, can play a significant role if the defect size is within certain limits.

It is discovered that the girth weld response to the remotely applied strain may be characterized by a three-region diagram. For a given set of defect size and weld strength mismatch conditions, the crack driving force may be bounded, unbounded, or gradually changing, with respect to the remotely applied strain. A set of parametric equations is developed that allow the computation of allowable strains with the input of defect depth, defect length, CTOD toughness, and weld strength mismatch.

The comparison of the developed strain criteria with full-scale bend tests and tensile-loaded CWPs (curved wide plates) shows the criteria are almost always conservative if lower bound CTOD toughness for a given set of welds is used. However, the criteria can significantly underpredict strain capacity of girth welds with short defects. Although defect length correction factors were added to the strain criteria based on the comparison of axisymmetric finite element (FE) results and full-scale bend test results, a more thorough investigation of the effects of defect length on strain capacity is needed. Future investigation that incorporates the finite length defects is expected to greatly reduce the underprediction. The influence of other factors, such as strain hardening rate, should be further quantified.

INTRODUCTION

Most girth weld defect assessment procedures are stress-based. Many geometry and material specific parameters can be neglected to conduct a reasonably accurate stress-based defect assessment. The simplicity of this method is typified by the widely used Level 2 assessment procedure in PD 6493:1991 [1], which is succeeded by BS 7910:1999 [2], in the oil and gas industries. However, there are some situations where stress-based defect assessment may not be appropriate. The longitudinal strains can greatly exceed the yield strains in pipelines through discontinuous permafrost, soil or seismic instability, and in offshore pipe laying. The stress-based assessment procedures are incapable of providing safe strain limits for such high strain conditions.

With the increased use of high-strength line pipes and associated greater likelihood of weld strength undermatching [3], it is important that the weld mismatch effects are accounted accurately. Possible weld strength undermatching

in modern pipelines cannot be effectively dealt with by stress-based assessment procedures when the nominal strain is beyond yield.

Limit states based design is gaining wider acceptance in the pipeline industries. The application of limit-states-based ECA (Engineering Critical Assessment) requires the accurate definition of various limit states. This is especially true in the view that most codified deterministic ECA codes are based on the philosophy of failure avoidance, not failure prediction [4]. The development of accurate deterministic strain design criteria should prove beneficial in establishing realistic limit states design methodology, as evident in the recent construction of two offshore arctic pipelines [5,6].

Strain limits pertaining to the tensile failure of girth weld defects have been applied in design and construction pipelines when the applied strain is beyond yield strain. As a general industry practice, 0.5% tensile strain limit has been used in pipe designs when certain toughness requirements are met. In some cases, higher strain limits have been justified through case-specific analysis and experimental verification [5,6]. The work presented in this paper is the initial efforts in understanding the various factors affecting the strain limits of girth welds containing welding defects. The intent of this work was to develop strain design guidelines of a limited range of applicability. It was envisioned that this range would be extended through future investigations.

STATUS OF PIPELINE ECA PROCEDURES IN RELATION TO STRAIN BASED DESIGN

A number of ECA procedures have been codified. API 1104 Appendix A is based entirely on fracture considerations [7]. Failure by plastic collapse is not considered. In CSA Z662:1996, both plastic collapse and fracture are considered [8]. The EPRG Guidelines on the Assessment of Defects in Transmission Pipeline Girth Welds adopted a rather unique approach [9]. It requires a girth weld meet certain minimum toughness values. Once this condition is satisfied, the defect limits are based solely on plastic collapse (gross and/or net section collapse). A three-tier approach is taken. Tier 1 is equivalent to workmanship criteria. Tiers 2 and 3 establish defect limits based on fitness-for-service (FFS) principles. The BS 7910:1999 [2] and R-6 Rev. 3 [10], along with their respective software, employ a failure assessment diagram (FAD) format in a multi-level approach. Plastic collapse and brittle fracture are simultaneously considered. An ECA procedure specially tailored to pipeline girth welds has been developed and validated against full-scale experimental test data [11,12]. This procedure incorporates the effects of weld strength mismatch in a stress-based FAD format.

In addition to the oil and gas industry, other industries have developed ECA codes and standards. For example, in the nuclear industry there are assessment procedures in Section XI of the ASME Boiler and Pressure Vessel Code for circumferential surface flaws [13]. These procedures were developed from large research programs, aimed at evaluating limit-load and elastic-plastic fracture solutions. The nuclear industry tends to use the *J*-integral fracture parameter rather than CTOD, but the two fracture parameters are related. Both analytical developments and experimental efforts have been extensive in the nuclear work [14, 15, 16]. The key differences between the efforts in the nuclear industry and the oil and gas industry is that the nuclear pipe has lower D/t and Y/T ratios. The methodologies in the nuclear industry, however, have considered both stress-based criteria (i.e., load-controlled loading as in the ASME Section XI criteria) and strain-based criteria (displacement-controlled loading).

Graville and Dinovitzer [17] attempted to develop strain-based failure criteria for part-wall defects in pipes. They used a modified Dugdale strip yield model to derive the maximum plastic extension of the ligament. A semi-empirical bulging factor was developed using FE analysis. When compared with experimental results, the model accurately predicted the failure stress. However, the predicted ligament extension did not agree with the more refined FE results at stress levels near or beyond general yield.

The recently updated DNV offshore standard [18] stipulates that ECA should be performed per Level 3 procedure of BS 7910:1999 [2] if the *accumulated plastic strain* is greater than 0.3%. Interestingly, no clear definition is given to the term accumulated plastic strain. The Level 3 procedure of BS 7910:1999 requires the material's *J* or CTOD resistance curve, instead of the CTOD toughness often used in the oil and gas industry, as one of the basic inputs for the ECA. There is very little published data on the application of the DNV offshore standard. It remains to be seen how well the Level 3 procedure of BS 7910 may be applied to high applied-strain conditions while recognizing that the fundamental basis of the Level 3 procedure is stress-based.

METHODOLOGY OF ESTABLISHING STRAIN DESIGN CRITERIA

Assessing the significance of weld defects by fitness-for-service (FFS) principles requires the knowledge of crack driving force and material's fracture toughness. The fracture toughness is generally obtained from laboratory specimen testing. The crack driving force is related to the magnitude of applied stress or strain, type of geometry, and size of the crack. The large library of available crack driving force solutions is almost entirely expressed in terms of applied stress. Examples of such crack driving force solutions are various stress intensity factory (K_I) solutions widely available in handbooks and publications and the GE/EPRI *J* solutions [19]. The only notable exception is the CTOD design curve [20,21] in which the crack driving force is expressed in terms of strain. However, the plastic part of the CTOD design curve is an empirical correlation based on test data of flat plates with through-wall cracks. Its accuracy is not sufficient for pipeline girth welds with surface-breaking or buried defects and weld strength mismatch.

Having crack-driving force in terms of applied strain is one of the most important steps in establishing an accurate strain design criteria. The next section describes the effort in understanding the relationship between crack driving force and the applied strain with defect size and weld strength mismatch as the contributing factors. The section that follows provides the parametric relations between the crack-driving force and the various contributing factors.

By setting the CTOD driving force equal to a CTOD toughness value, the critical strain of a defect is determined. The last part of this paper compares the critical strains with the available experimental data.

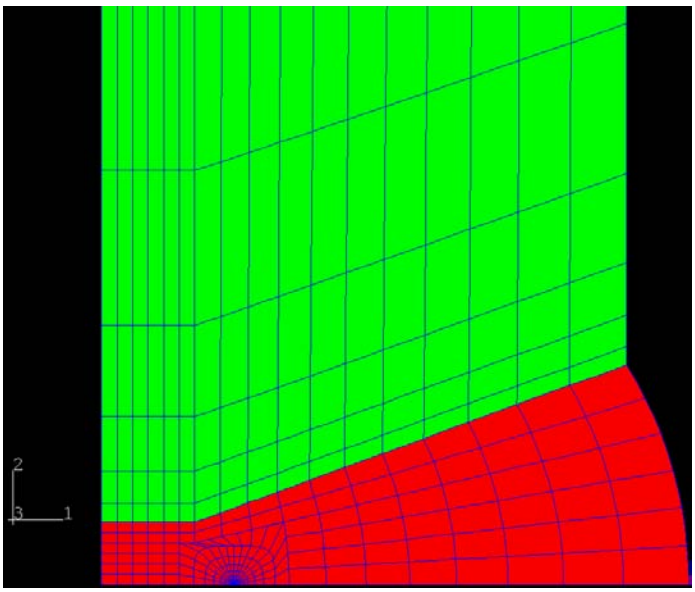

Figure 1 FE mesh representing the cross-section of a girth weld with an internal crack

CRACK-DRIVING FORCE FROM FE ANALYSIS

Description of FE Procedures

As the first concerted effort in understanding the effects of various parameters on the strain limits of girth welds, the FE analyses are simplified to axisymmetric models similar to that shown in Figure 1. The defect depth and weld strength mismatch are the primary variables. The other parameters are given as follows:

- Diameter: 1069 mm (42 inch)
- Wall thickness (t): 13.4 mm (0.528 inch)
- Base metal yield strength (σ_y^B): 620.5 MPa (90 ksi)
- Weld strength mismatch ($M = \sigma_y^W/\sigma_y^B$): $M = 0.7$ to 1.5 at increment of 0.1
- Y/T : 0.90
- Crack depth (a):14 values, approximately from 6% to 90% of the wall thickness
- Crack length: fully circumferential (axisymmetric analysis)
- Crack location: center of weld
- Weld cap height: 0 and 1.59 mm (1/16 inch)
- Weld land length: 2.38 mm (3/32 inch)
- Bevel angle: 20 degree
- Root gap: 3.18 mm (1/8 inch)

Other than the multiple defect depths and two weld cap heights, all other geometric parameters were kept constant. The FE meshes were generated by a mesh generator that was capable of generating multiple input files in the ABAQUS® format.

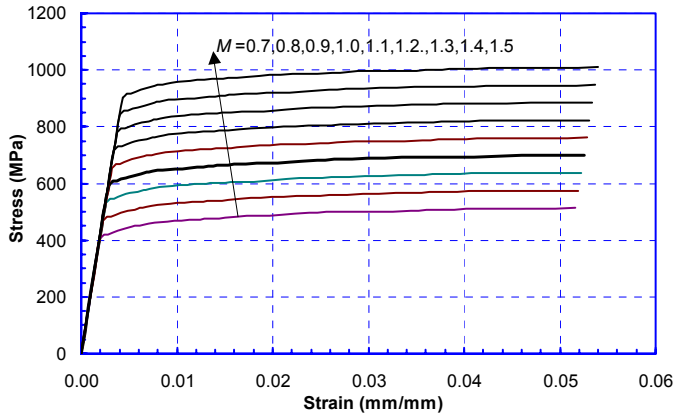

Figure 2 Assumed engineering stress strain curves of the pipe material and the weld metals for the parametric analyses. The thick solid line is the pipe material (M=1.0).

The base metal stress strain curve was held constant. The weld strength mismatch was achieved by adjusting the weld metal yield and tensile stresses of a fixed amount. The full stress strain curves of the pipe and weld metals are shown in Figure 2.

With the listed ranges of defect depth, weld strength mismatch level, and weld cap height, a total of 252 cases of FE analysis were performed. With the aid of the mesh generator and an automated post-processing routine, this large number of analyses was completed in a reasonable time period.

Eight-node axisymmetric elements (CAX8R in ABAQUS®) were used. Uniform axial displacement was applied at the end of the model far from the girth weld. The crack tip was modeled using collapsed elements to simulate the crack tip stress singularity. The CTOD driving force at any given strain level was computed from the crack tip deformation profile using a customary 45^0 interception method by a data post-processing program [22].

Finite Element Analysis Results

The primary output of the parametric FE analysis was the relationship between the CTOD driving force and the applied nominal strain for a wide range of crack depth and weld strength mismatch levels. The applied nominal strain is the longitudinal strain on the pipe material remote from the girth welds.

Figure 3 shows the typical relations between the CTOD and the applied nominal strain for girth welds with different crack depths. The crack depths ranged from 6% to 89.6% of the pipe wall thickness. The weld strength mismatch ratio was 1.0 and the weld cap height was 1.59 mm.

The variation of the CTOD in response to the applied nominal strain can be characteristically divided into three regions. In Region 1, represented by the almost vertical lines, the increase of the CTOD is immediate over the increase of the applied nominal strain. Indeed, the rise of the CTOD is almost unbounded beyond certain strain levels. This phenomenon is the manifestation of highly localized strain concentration at the girth weld because of the large crack depth. In Region 3, represented by the almost horizontal lines, the increase of the CTOD driving force is very small over the large increase in the applied nominal strain. There is no strain concentration across the girth weld because the crack depth is small.

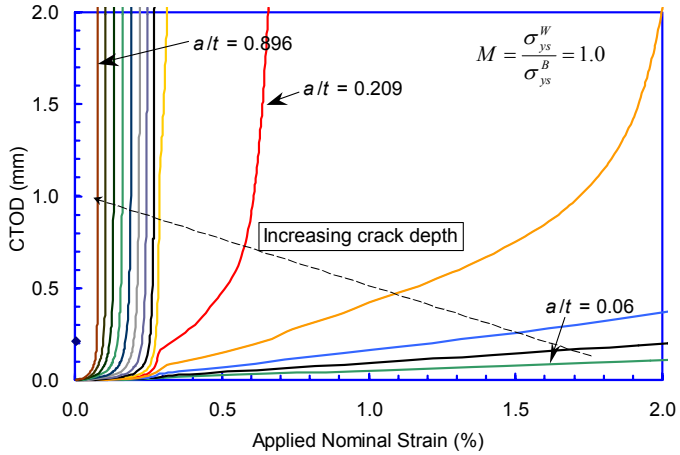

Figure 3 Relations of the CTOD driving force and the applied nominal strain of a girth weld with internal cracks of various depths

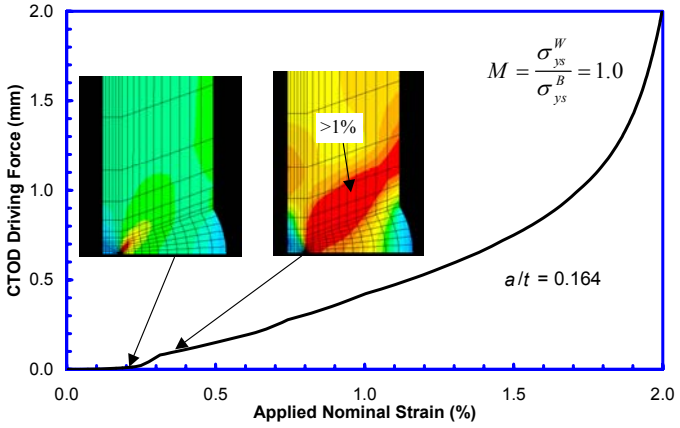

Figure 4 Evolution of the crack-tip plasticity with the increase of applied nominal strain for a girth weld with moderately deep defect

In the Region 2 bounded by Regions 1 and 3, the increase in CTOD with the nominal strain is gradual and complex interactions exist between weld and the base pipe material. An example of Region 2 response at the crack depth of a/t = 0.164 is illustrated in Figure 4. When the nominal strain is less than 0.25%, the overall CTOD response is essentially elastic. The strain at the crack tip is high, but the high strain does not reach the back surface of the pipe. At an applied nominal strain of 0.25% to 0.30%, an up-turn in the CTOD response is observed. This is the point when the high strain starts to reach the back surface (OD) of the pipe. Subsequent strain hardening in the girth weld region beyond the nominal strain of 0.3% forces a uniform strain distribution between the weld and pipe material. Eventually, at nominal strain of approximately 2.0%, the strain hardening in the girth weld can no longer offset the strain hardening in the pipe material, high strain concentration across the girth weld occurs. A rapid rise in CTOD is seen at this strain level.

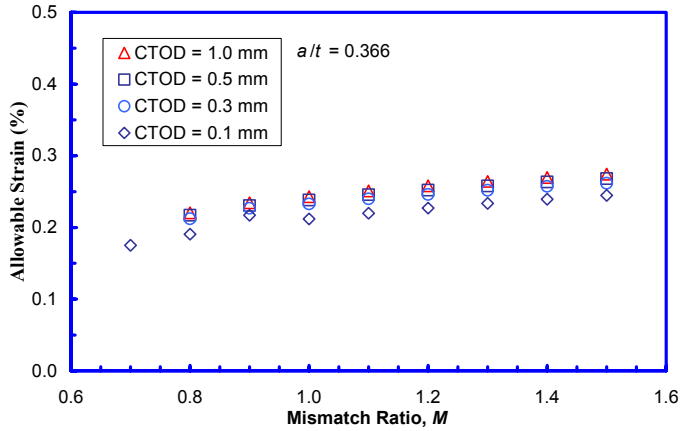

Figure 5 Allowable strains as functions of weld strength mismatch ratio at various assumed CTOD toughness levels for a relatively deep crack

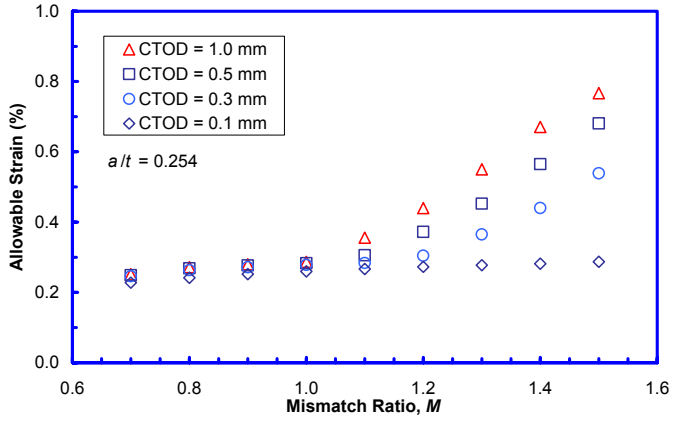

Figure 6 Allowable strains as functions of weld strength mismatch ratio at various assumed CTOD toughness levels for a moderately deep crack

By setting the CTOD driving force to an assumed CTOD toughness value, the relations similar to that shown in Figure 3 can be used to derive the allowable strains for given values of CTOD toughness. Examples of allowable strain as functions of CTOD toughness and weld strength mismatch are given in Figure 5 to Figure 7.

Figure 5 represents a case of a relatively deep crack. With even a small nominal strain, the crack tip plasticity quickly spreads to the back surface of the pipe wall. The rise of the applied CTOD at the crack tip is immediate and almost unbounded, seen as vertical lines in Figure 3. As a result, the allowable strains are not affected by the CTOD toughness and weld strength mismatch.

Figure 6 shows a case of an intermediate flaw depth. When the mismatch ratio is less than 1.0, the allowable strain is not affected by the CTOD toughness. This condition is essentially the same as that represented by Figure 5 when the rise of CTOD driving force is immediate and almost unbounded. At higher mismatch ratios, higher CTOD toughness provides higher allowable strains. As compared with the low mismatch condition, the strain concentration across the girth weld becomes less with the higher mismatch level.

Figure 7 shows a case of a shallow crack. The allowable strain is strongly affected by both CTOD toughness and weld strength mismatch level. At a mismatch ratio of 1.0, a factor of 10 increase in the CTOD toughness yields a factor of 6 increase in the allowable strain.

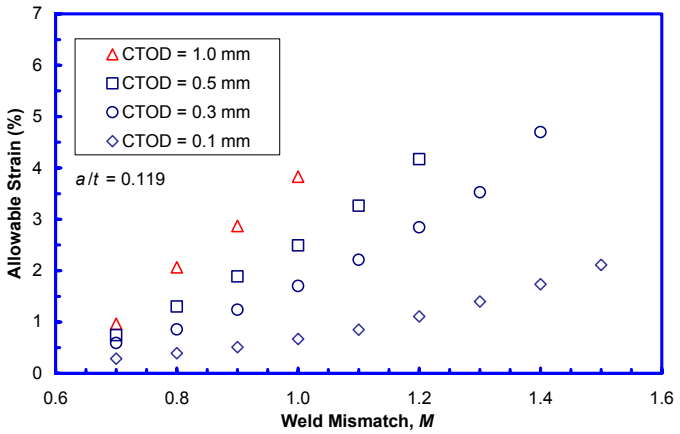

Figure 7 Allowable strains as functions of weld strength mismatch ratio at various assumed CTOD toughness levels for a shallow crack

It may be concluded from Figure 5 to Figure 7 that the strain limits of girth welds are a result of complex interactions of various contributing factors. The process of such interactions is best viewed through the pattern of crack-tip plasticity development. When the crack is deep, the crack-tip plasticity cannot be contained. The resulting strain concentration in the cracked plane leads to asymptotic increase in crack driving force. The strain limits under such conditions are low regardless the toughness and mismatch levels.

When the crack depth is smaller than a critical size, fracture toughness and weld strength mismatch starts to play an important role. For the cases shown in Figure 7, achieving a strain limit of 1% would require a mismatch level of 1.15 if the CTOD toughness were 0.1 mm. At the same mismatch level, a strain limit of 2.5% may be achieved if the CTOD toughness is 0.3 mm.

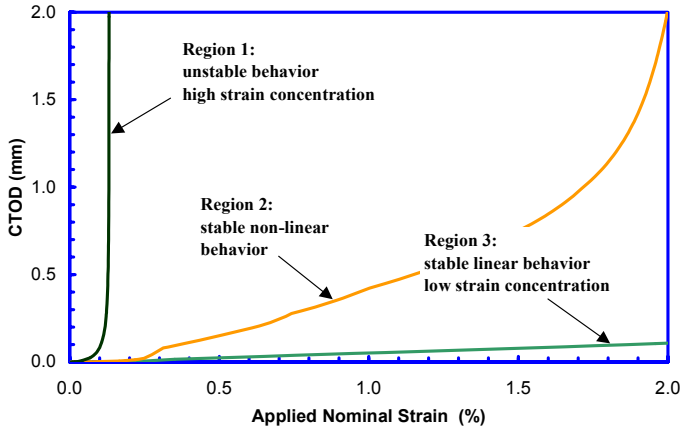

Figure 8 Illustration of the characteristics of the CTOD driving force versus applied strain response that forms the basis for the three-region strain design diagram

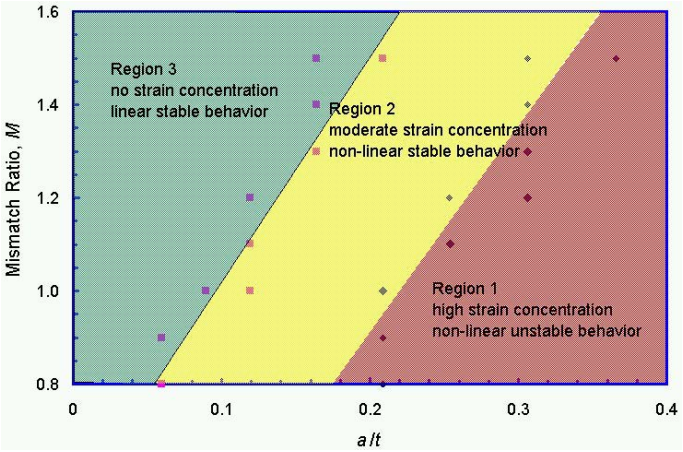

Figure 9 The three-region strain design diagram

A Three-Region Strain Design Diagram

The results of the previous section suggest that the CTOD driving force and applied strain relationships can be broken into three regions, see Figure 8. In Region 1, representing deep defects, a small increase of the applied strain results in a large rise in CTOD crack driving force. A large strain concentration occurs at the girth weld. In Region 2, representing intermediate defect depths, the increase of CTOD driving force is small until the crack-tip plastic strain reaches the back surface. This is followed by a rapid rise in CTOD

driving force with the increase of the applied strain. In Region 3, representing shallow defects, the increase of the CTOD driving force is small with a large increase in the applied strain. The high plastic strains are localized near the crack tip and the averaged strain in the girth weld is approximately the same as the rest of the pipe. The distinctive features of these three regions lead to the formation of the three-region strain design diagram of Figure 9.

The main feature of Region 1 is its unbounded increase in the CTOD driving force. In contrast, the main feature of Region 3 is that the crack driving force seems to saturate at a level. Region 2 is characterized by the gradual increase of the crack driving force with respect to the applied strain. The three regions of crack driving force behavior are categorized in terms of crack depth and weld mismatch level. At a given mismatch level, the CTOD driving force and the applied strain responses change abruptly from one region to the other with the change of the crack depth. When the mismatch level changes, the transition point in terms of crack depth varies. To define the precise transition point, very fine increments of crack depth are needed. The data scatter around the transition lines in Figure 9 indicates that the current increment size of defect depth is somewhat too coarse. In addition to crack depth, there may be other factors that affect the transition lines. Further analysis is needed to refine the transition lines in the three-region diagram.

The three-region diagram of Figure 9 may be used for preliminary strain design. It, however, does not provide strain limits. For example, for an internal crack depth of 10 percent of the wall thickness, a yield strength mismatch greater than 1.0 (overmatching) is required to assure that the strain response is stable and linear up to 2% strain (Region 3). The same strain limit may be achieved with a slightly undermatched weld (M<1.0) that has good fracture toughness (Region 2). For a typical mismatch level of 1.1, the maximum crack depth is approximately 25% of the wall thickness to avoid Region 1 behavior.

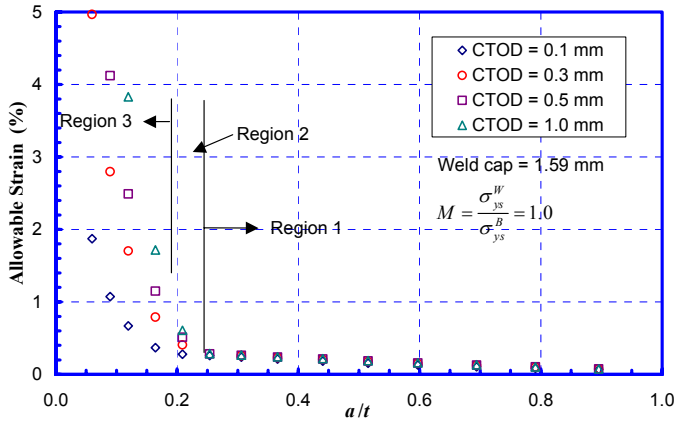

Figure 10 Example plot showing the relations between the allowable strain and the crack depth at various assumed CTOD toughness levels

Parametric Strain Design Relations

The three-region diagram may be constructed in a form like Figure 10 at a given mismatch level. The parametric strain design relations were developed through a series of curve fits to the relations similar to those of Figure 10.

Fitted Parametric Equations

The results of the 252 FE runs were fitted in the three regions due to their distinct features. The transitional region (Region 2) was not directly fitted with its equations, but a combination of the Region 3 and Region 1 fitted equations was used.

The allowable stress of Region 3 is given as,

$$\varepsilon_f^{(R3)}(\%) = \left(0.0278\mathrm{e}^{-2.099\delta}\right)\left(\frac{M^3}{1.119}\right)\left(\frac{a}{t}\right)^{-3.358\delta^{0.347}}, \qquad (1)$$

where ε_f^{R3} is the Region 3 allowable strain or strain limit of a girth weld and δ is the CTOD toughness.

The allowable strains of Region 1 is given as,

$$\varepsilon_f^{R1}(\%) = \frac{\left(-0.211\cdot\ln\left(\frac{a}{\mathrm{t}}\right)+0.0675\right)M^{0.22}}{1.119}, \quad \text{if} \quad \delta>0.5 \qquad (2a)$$

$$\varepsilon_f^{R1}(\%) = \frac{\left(-0.0442\delta-0.161\right)\ln\left(\frac{a}{t}\right)+0.00091\cdot\ln(\delta)+0.0677M}{1.119},$$

$$\text{if} \quad 0.05<\delta<0.5 \qquad (2b)$$

$$\varepsilon_f^{R1}(\%) = \frac{\left(-0.0228\cdot\ln(\delta)-0.202\right)\cdot\ln\left(\frac{a}{t}\right)+\left(-12.497\delta^2+2.085\delta\right)}{1.119}$$

$$\text{if} \quad \delta<0.05 \qquad (2c)$$

The allowable strain of Region 2 is given as,

$$\varepsilon_f^{R2} = \varepsilon_f^{R1} \quad \text{if} \quad a/t<0.05, \qquad (3a)$$

$$\varepsilon_f^{R2} = \varepsilon_f^{R3} \quad \text{if} \quad 0.05 < \frac{a}{t} < \frac{0.110\delta+0.191}{1.119}\cdot\left(\frac{t_w}{t_b}\right), \qquad (3b)$$

$$\varepsilon_f^{R2} = \varepsilon_f^{R1} \quad \text{if} \quad \frac{a}{t} \ge \frac{0.110\delta+0.191}{1.119}\cdot\left(\frac{t_w}{t_b}\right), \qquad (3c)$$

where t_b is the pipe wall thickness and t_w is the maximum wall thickness of the weld, i.e., the pipe wall thickness plus the weld cap height.

Figure 11 shows that the fitted equations agree well with the FE results for the case of M=1.0. Figure 12 shows that the Region 3 equations provide good agreement with the FE results of a/t=0.1194. Similarly good agreement is evident in Figure 13 for relatively deep cracks at a/t=0.3657. In this region, the allowable strain remains small regardless the

CTOD toughness and weld strength mismatch ratio. The fitted equations predict the FE results at the small and large values of CTOD but slightly under-predict the strain for intermediate values of CTOD. However, since the change in strain with increasing mismatch ratio in this region is small, these under-predictions are of little consequence. Figure 14 shows that the fitted equations provide overall good agreement with the FE results for an intermediate crack depth in the transition region. There is a slight under-prediction at the large CTOD values and a slight over-prediction at the mid CTOD values.

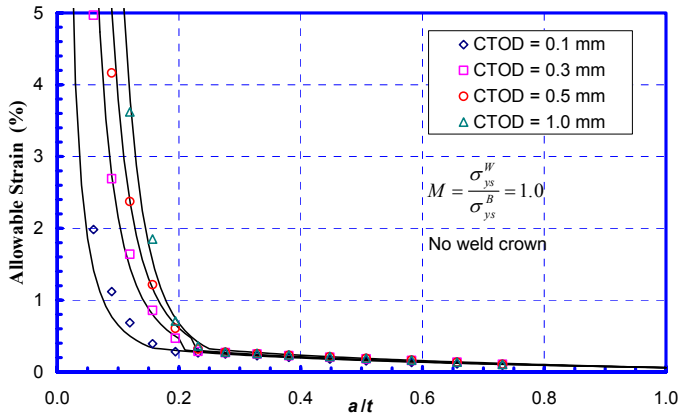

Figure 11 Comparison of FE results (represented by the individual symbols) and the fitted parametric equations (represented by the lines)

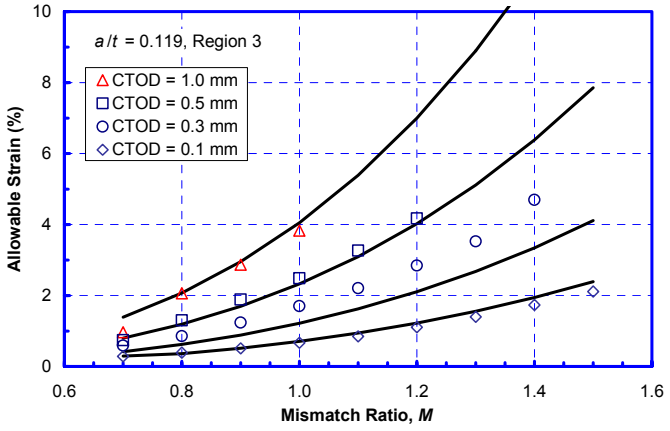

Figure 12 Comparison of the FE results (symbols) and the fitted parametric equations (lines) for Region 3 defects

As evident in Figure 14, the fitted equations tend to be less accurate in Region 2 at high mismatch ratios. This inaccuracy is the results of limited amount of data in the transitional region that can be used for curve fit. To define the transition region more precisely, additional analyses with finer increments of defect depth are required. At high mismatch ratios, the abrupt change from Region 1 to Region 3 behavior leaves very few data points in the transition region (Region 2), see Figure 15. A smaller increment of *a*/*t* would have produced more data points in Region 2.

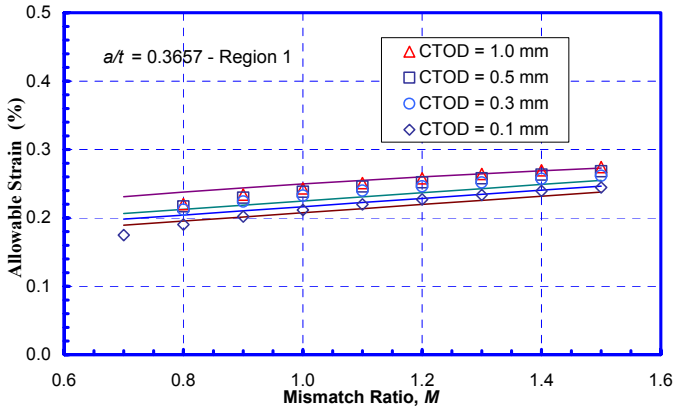

Figure 13 Comparison of the FE results (symbols) and the fitted parametric equations (lines) for Region 1 defects

EXPERIMENTAL VERIFICATION

The strain design criteria described above are based on a large number of FE analyses that include a limited number of variables. Girth welds produced under field welding conditions have considerably more variables. Consequently, the strain limits can vary even for nominally the same welds. This section describes the validation of the newly developed strain design criteria.

Validation against Full-Scale Test Data

Description of the Full-Scale Tests

In the early 1980's, the fracture behavior of pipeline girth welds was investigated though an extensive full-scale experimental test program conducted at the University of Waterloo and the Welding Institute of Canada (WIC) [23,24,25]. Most of the tested pipes were API Grade X70 (483 MPa), a few were X65 (448 MPa) and X60 (414 MPa) grades. The diameter of the pipes ranged from 20 inch (508 mm) to 42 inch (1067 mm). The reported CTOD toughness was in the range of 0.03 to 0.10 mm (0.0012 to 0.0039 inch). The bending moments, stresses, and remote nominal strains at the critical events were reported for many of these tests. The critical events could be brittle fracture, brittle fracture after ductile tearing, buckling, or manual intervention. Failure strains were not recorded in some of the tests. Thirty-five (35) of these tests with reported strains are used for comparison here.

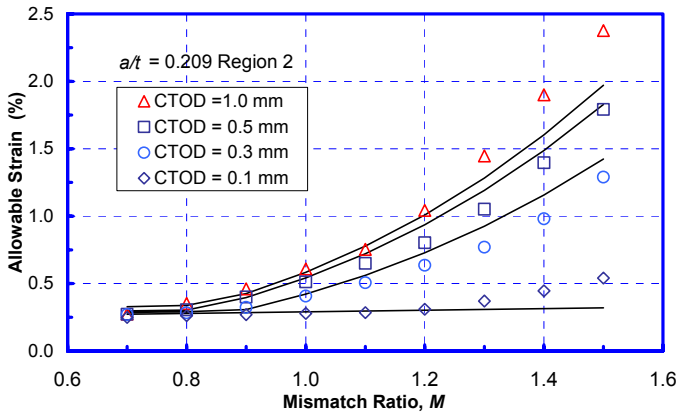

Figure 14 Comparison of the FE results (symbols) and the fitted parametric equations (lines) for Region 2 defects

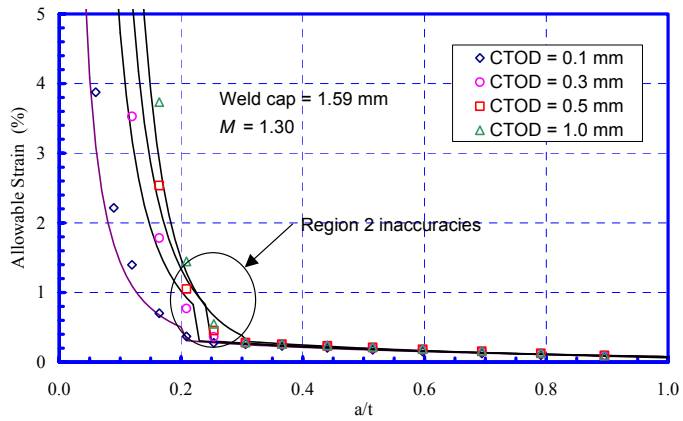

Figure 15 More data points in Region 2 for the highly overmatched welds would have allowed more precisely fitted equations.

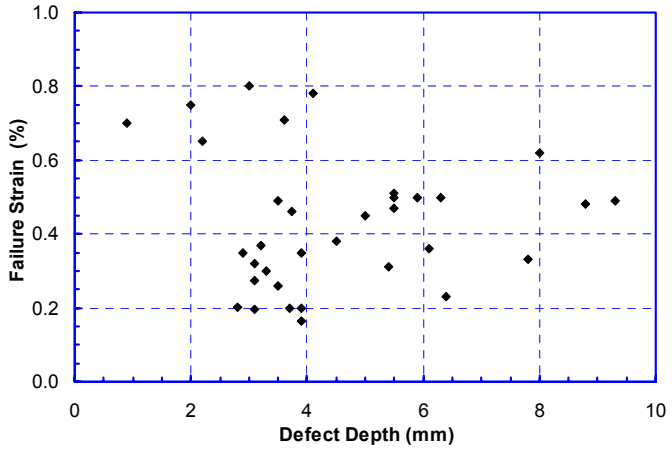

Figure 16 Failure strain from the full-scale tests as a function of the defect depth

Figure 16 shows the failure strains measured from the full-scale tests as a function of the defect depth. When the defect depth is less than approximately 2.7 mm, the failure strains are generally high, although the three data point may not be considered as a general trend. However, the overall trend is not very clear. When the same data is plotted against relative defect depth, the trend becomes much clearer, see Figure 17. The failure strains appear to rise with the decrease of the relatively defect depth.

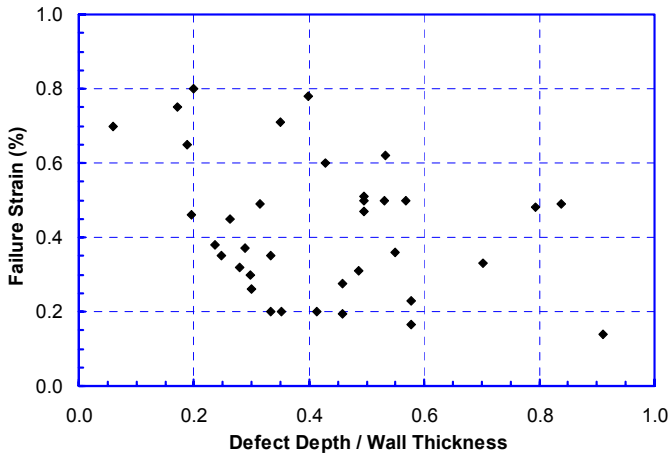

Figure 17 Failure strain from the full-scale tests as a function of the relative defect depth

Comparison with Full-Scale Test Data

To apply the parametric strain criteria, the following input variables are needed:

- Defect depth
- CTOD toughness, and
- Weld strength mismatch.

Among those variables, the weld strength mismatch levels were unknown. For the Grade X70 and X65 pipes tested, it is reasonable to assume a moderate level of overmatching. A constant mismatch level of 1.1 was assumed for all the cases. With the actual defect depth and CTOD toughness, the allowable strains were computed using Eqs. (1)-(3).

A comparison of the failure strains from the full-scale tests with the predicted failure strains of the parametric formulae is shown in Figure 18. The *y*-axis represents the ratio of experimentally measured failure strain over the estimated failure strain using Eqs. (1)-(3). In almost all the cases, the parametric formulae predicted the lower bound failure strain for the same relative defect length. There appears a rise in the strain ratio when the relative defect length is less than 0.05.

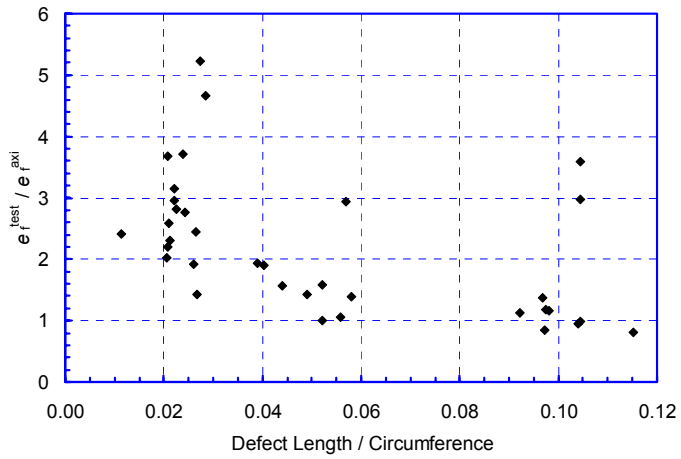

Figure 18 Comparison of the failure strains from the full-scale tests and the predicted failure strains from the fitted parametric equations

Defect Length Correction Factor

Data shown in Figure 18 formed the basis for a tentative defect length correction factor. When the relative defect length is less than 0.05, a lower bound correction factor may be expressed as,

$$\frac{e_f}{e_f^{axi}} = 2 - \frac{\beta}{0.05} \quad \text{if} \quad \beta<0.05, \tag{4a}$$

$$\frac{e_f}{e_f^{axi}} = 1 \quad \text{if} \quad \beta\geq 0.05, \tag{4b}$$

where β is the relative defect length (defect length / circumference), e_f is the failure strain of a finite length defect, and e_f^{axi} is the failure strains from Eqs. (1)-(3), i.e., axisymmetric results. The maximum increase of failure strain for a finite length defect over a fully circumferential defect is 2, when the defect length approaches zero.

A correction factor going through the middle of the experimental data may be expressed as,

$$\frac{e_f}{e_f^{axi}} = 4 - 3\frac{\beta}{0.05} \quad \text{if} \quad \beta<0.05, \tag{5a}$$

$$\frac{e_f}{e_f^{axi}} = 1 \quad \text{if} \quad \beta\geq 0.05. \tag{5b}$$

The maximum increase in failure strains by applying the correction factor of Eq. (5) is 4 at zero defect length (β=0), as compared to those from Eqs. (1)-(3).

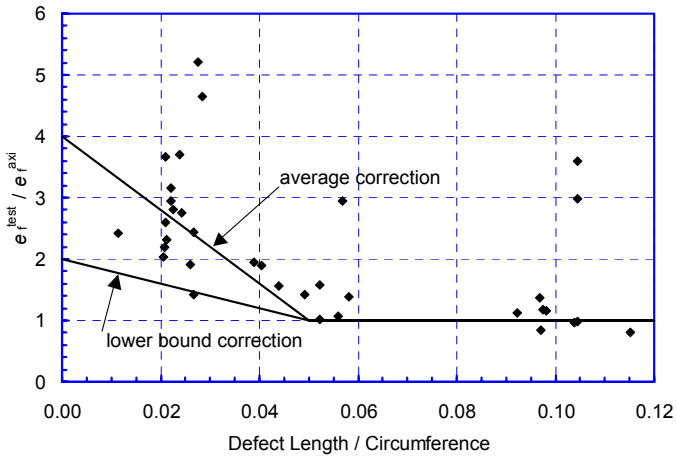

Figure 19 Comparison of the proposed defect length correction factors with the full-scale test data

It should be emphasized that Eqs. (4) and (5) are based on a limited number of full-scale test data. Even with the defect length correction factors of Eqs. (4) and (5), the current strain criteria underestimate the strain limits for short defects. It is shown in Figure 16 and Figure 17 that the lower bound strains at β>0.05 is approximately 0.2%. The axisymmetric criteria of Eqs. (1)-(3) predict these lower bound values well. The maximum defect length correction factors are 2 and 4 from Eq. (4) and Eq. (5), respectively. Therefore, the maximum predicted strain limits are 0.4% as a lower bound value and 0.8% as an averaged value, even when the defect length approaches zero (no defects). In reality, a girth weld of reasonable toughness and with no defects can have a strain limit of a few percent. The effects of defect length on the strain limits need further investigation, especially for short defects

Validation against Curved Wide Plate (CWP) Test Data

The comparison of full-scale pipe and curved wide plate (CWP) tests has demonstrated that tensile loaded CWPs fail at lower strain and stress levels than the full-scale pipe under bending. Therefore, the results of CWP tests are considered conservative relative to the full-scale behavior. The failure characteristics of a flawed girth weld subject to bending can be approximated from the failure characteristics of a tensile loaded CWP.

Description of the CWP Database

The entire Laboratory Soete CWP database contains 356 fully documented test results of single flawed specimens. The remote failure strains of these specimens are given in Figure 20. In addition to the CWP tests, the pipe and girth welds were subjected to pipe metal tensile (axial direction), hardness, all-weld metal tensile, Charpy V impact, and CTOD testing. The Charpy and CTOD toughness properties were measured at the weld metal centerline. In most cases, the full

transition curves of Charpy and CTOD are available. All CWP specimens were tensile loaded to failure or interrupted at maximum load. For each CWP test, a range of information is documented, including the failure stress and strain and the load and deformation behavior, as visualized by the Moire technique at specimen failure or at maximum load. The full details of the database cannot be disclosed here due to commercial confidentiality.

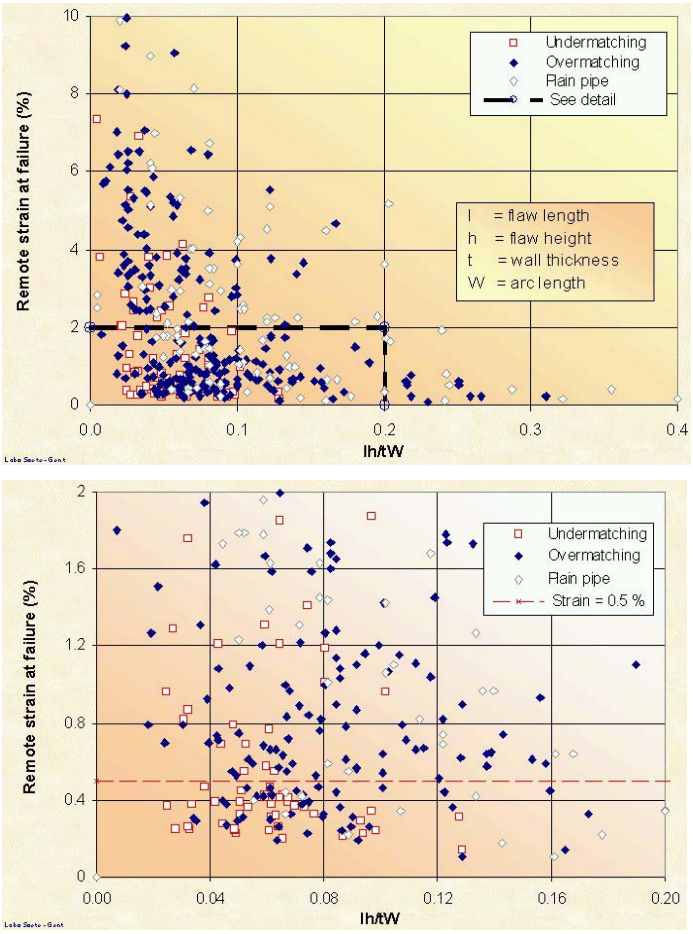

Figure 20 Remote failure strains as a function of the relative cross-sectional area. The lower figure provides the detailed view of the lower strain range of the upper figure.

For the current validation, a subset of 64 CWP test results was selected randomly so that a wide range of relevant variables was available. The specimen were extracted from large diameter pipes of 36 to 48 inches OD, a wall thickness range of 0.267 to 1.14 inch (6.8 to 28.9 mm), pipe grades from X60 to X80 with most of the data being for X70, a CTOD range (mean values, at CWP test temperature) of 0.07 to 0.69 mm (2.8 to 27.0 mils), and a pipe metal Y/T of 0.90 to 0.79.

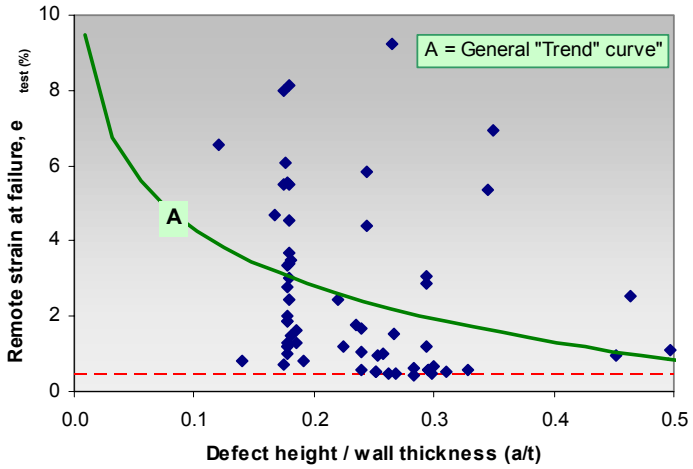

Figure 21 Remote failure strains from 64 CWP tests as a function of relative defect depth

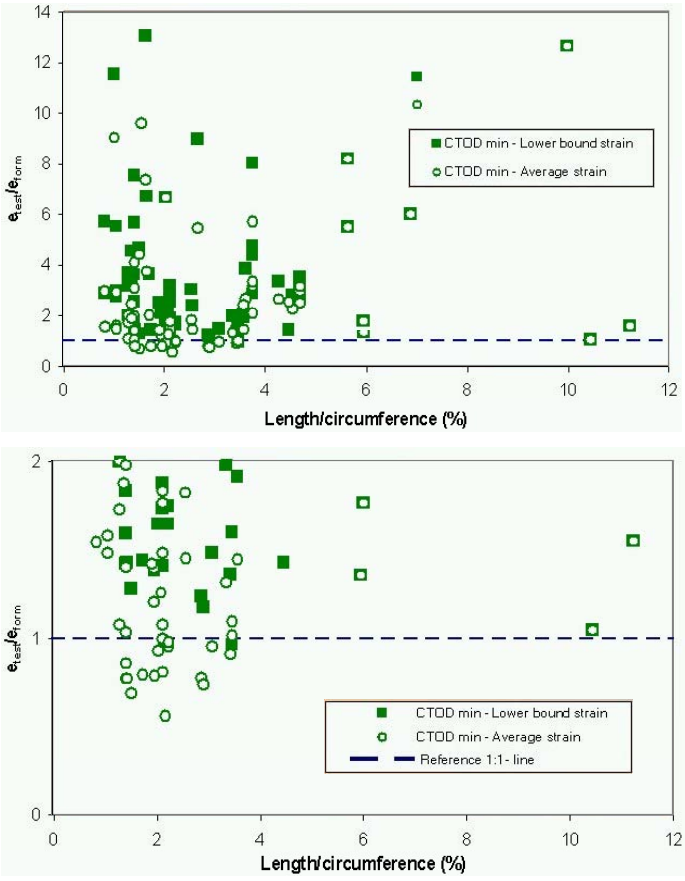

Figure 22 Comparison of the calculated and measured remote failure strains of the CWP specimens. The minimum CTOD toughness was used in the computation.

Comparison with CWP Test Data

The remote failure strains of the 64 CWP specimens are given in Figure 21 as a function of the relative defect height (a/t). The thick line represents the approximate trend of the data and the broken line is at 0.5% strain level. As compared to the full-scale test results of Figure 17, the CWP database contains a large number of tests with the remote failure strains exceeding 1%. As expected, the relationship between the remote failure strain and relative defect depth is far from unique. The observed scatter is attributable to a range of factors, including toughness, weld strength mismatch, and Y/T ratio. The deformation behavior and straining capacity of a flawed girth welds is affected by a large number of parameters and the interaction between the weld and pipe metals.

The variables needed to assess the preliminary strain criteria of Eqs. (1)-(5) are defect depth, CTOD toughness, and the yield strength mismatch. The current database covers a wide range of those variables. The allowable strains computed from a piece of software that incorporates the Eqs. (1)-(5) are compared with the experimental values, see Figure 22 and Figure 23. The estimated failure strain from Eqs. (1)-(5) is denoted by e_{form}. The average (open circles) and lower bound (solid squares) strains were computed from the software using both minimum and mean CTOD values.

Observation of the CWP Validation

It may be observed from Figure 22 and Figure 23 that the predicted lower bound allowable strains (solid symbols) are conservative ($e_{test}/e_{form} > 1$). The predicted averaged strains are "non-conservative" for several tests (open symbols). In addition, the scatter of the predictions is quite significant.

There are a number of possible contributing factors to the non-conservative predictions of the newly developed strain criteria with respect to some CWP test data. The failure strains from tension-loaded CWPs are generally lower than those from full-scale pipes under bending. This underestimation from the CWP tests is greater for plates containing long defects because the net section area is proportionally less. Therefore, one of the possible contributing factors to the "non-conservative" predictions could be the underestimation of failure strains of the CWP tests. While this underestimation is conservative in deterministic defect assessment, it may have exaggerated the "non-conservatism" of some of the predicted failure strains. Further investigations are needed to valid this possibility, along with the consideration of other possible contributing factors.

The EPRG Tier 2 guidelines on girth weld defect acceptance criteria limit defect area to less than 7% in any 300 mm length of weld [9,26]. The wide plate test results show that girth welds containing defects smaller than this limit fail by plastic collapse with remote failure strains greater than 0.5%, provided the weld metal is matching or overmatching and the mean value of weld metal toughness is greater than 30 ft-lb (40 J). The Tier 2 guidelines are limited to line pipes with Y/T≤0.9. Some modern pipelines are expected to have design strains well over 0.5% while using linepipe materials with Y/T ratios greater than 0.9 and possibly under slightly undermatching conditions. It is therefore necessary to define requisite conditions of achieving failure strains much greater than 0.5% under modern field welding conditions for high-strength line pipes.

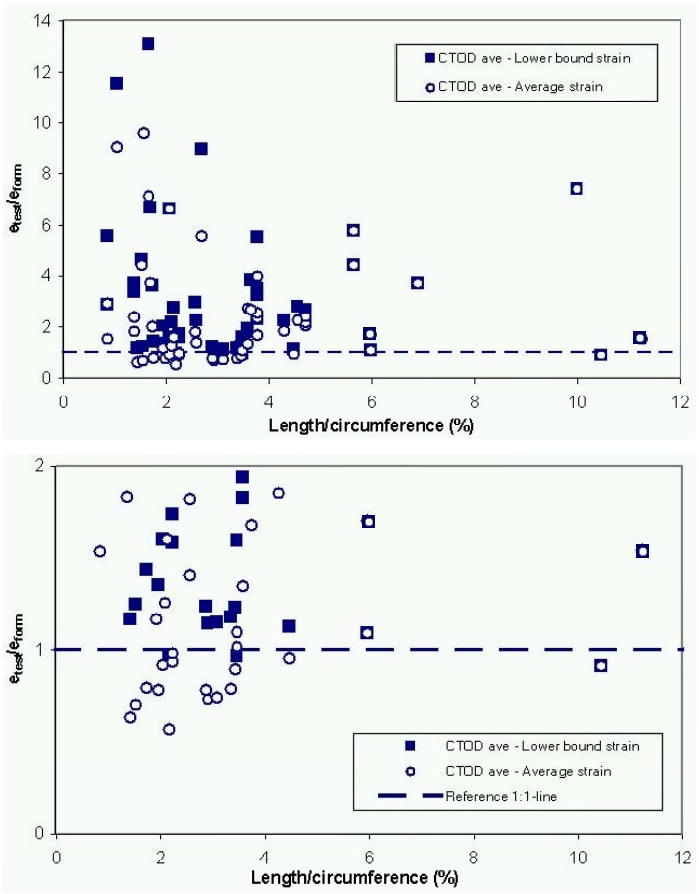

Figure 23 Comparison of the calculated and measured remote failure strains of the CWP specimens. The mean CTOD toughness was used in the computation.

CONCLUDING REMARKS

The strain capacity of girth welds is examined through numerical analysis and the application of available experimental data. Important insights on the various factors affecting the girth weld strain capacity are generated. The defect size is identified as one of the most dominant factors in determining strain capacity of a girth weld. Other factors, such as the strain hardening rate of the pipe and weld metals, weld strength mismatch, fracture toughness, and weld cap height, can play a significant role if the defect size is within certain limits.

As an initial effort in addressing the very complex issue of strain design criteria, this work provides a conceptual

description of the strain design methodology in the form of the three-region design diagram. The parametric strain design procedure of Eqs. (1)-(5) can be useful in evaluating the influence of defect size and mismatch level on the strain limits of girth welds. A number of important contributing factors to strain limits, such as strain hardening rate, is not included in the parametric procedure. These limitations should be considered when using the parametric procedure. Furthermore, the work described in this paper only considers the weld centerline defects. The work is under way in another PRCI supported project to examine the strain design criteria of HAZ defects.

The comparison of the developed strain criteria with full-scale bend tests and tensile-loaded CWPs shows the criteria are almost always conservative if lower bound CTOD toughness for a given set of welds is used. However, the criteria can significantly underpredict strain capacity of girth welds with short defects. Although defect length correction factors were added to the strain criteria based on the comparison of axisymmetric FE results and full-scale bend test results, a more thorough investigation of the effects of defect length on strain capacity is needed. A future investigation that incorporates the finite length defects is expected to greatly reduce the underprediction. The influence of other factors, such as strain hardening rate, should be further quantified. Given the experimentally observed scatter in failure strains of nominally the same welds, a relatively large range between the predicted failure strains and the actual failure strains may always exist.

The strain-based design is most useful under high strain conditions. To achieve strain limits much greater than 0.5% in modern high-strength line pipes, the allowable defect size is likely to be small. Therefore, further work in the development of strain-based ECA procedures should focus on small and yet detectable defects. The weld strength mismatch and Y/T ratio are likely to play an important role in ensuring high strain limits when the defects are small. The strain hardening capacity of the base metal and weld metal can be different. These different strain hardening capacities may cause their stress strain curves to intersect. These factors are being examined in a follow-on PRCI funded project.

ACKNOLEDGMENT

The financial support of PRCI is greatly appreciated. The assistance of Dr. Zhili Feng of Emc^2 in formatting this paper proved very beneficial.

REFERENCES

1 BSI PD 6493:1991, "Guidance on Methods for Assessing the Acceptability of Flaws in Fusion Welded Structures."

2 BS 7910:1999, "Guide on Methods for Assessing the Acceptability of Flaws in Metallic Structures," British Standards Institution, 1999.

3 Glover, A. G., Horsley, D. J., and Dorling, D. V., "High-Strength Steel Becomes Standard on Alberta Gas System," in *Oil and Gas Journal*, Vol. 97, No. 1, Pennwell, 1999.

4 Pisarski, H. G., "Comparison of Deterministic and Probabilistic CTOD Flaw Assessment Procedures," Proceedings of 17th International Conference on Offshore Mechanics and Arctic Engineering, Materials Symposium, Lisbon, Protugal, ASME, 1998.

5 Lanan, G. A., Nogueira, A.C., Even, T. M., and Ennis, J. O., "Pipeline Bending Limit State Design for the Northstar Offshore Arctic Development Project," Proceedings of Pipeline Welding and Technology, David Yapp, Ed., Galveston, Texas, October 26-28, 1999.

6 Nogueira, A. C., Lanan, G. A., Even, T. M., and Hormberg, B. A., "Experimental Validation of Limit Strain Criteria for the BPXA Northstar Project," Proceedings of Pipeline Welding and Technology, David Yapp, Ed., Galveston, Texas, October 26-28, 1999.

7 API 1104, "Welding of Pipelines and Related Facilities," API Standard 1104, Nineteenth Edition, September 1999.

8 CSA Z662-96, "Oil and Gas Pipeline Systems," Canadian Standards Association, December 1996.

9 Knauf, G, and Hopkins, P., "The EPRG Guidelines on the Assessment of Defects in Transmission Pipeline Girth Welds," 1996.

10 Milne I., Ainsworth, R, A., Dowling, A. R., and Stewart, A. T., "Assessment of the Integrity of Structures Containing Defects," CEGB R6, Rev. 3, May 1986.

11 Wang, Y.-Y., Rudland, D., Horsley, D., "Development of a FAD-Based Girth Weld ECA Procedure, Part 1 Theoretical Framework," Proceedings of the 4th International Pipeline Conference, Calgary, Alberta, Canada, September 29-October 3, 2002.

12 Wang, Y.-Y., Rudland, D., Horsley, D., "Development of a FAD-Based Girth Weld ECA Procedure, Part 2 Experimental Verification," Proceedings of the 4th International Pipeline Conference, Calgary, Alberta, Canada, September 29-October 3, 2002.

13 ASME Section XI Code, Appendix H, "Evaluation of Flaws in Ferritic Piping," ASME Boiler & Pressure Vessel Code, 1995.

14 Scott, P. M., and Ahmad, J., "Experimental and Analytical Assessment of Circumferentially Surface-Cracked Pipes Under Bending," NUREG/CR-4872, April 1987.

15 Krishnaswamy, P., Scott, O. Mohan, R., Rahman, S., Choi, Y. H., Brust, F., Kilinski, T., Francini, R., Ghadiali, N., Marschall, C., Wilkowksi, G., "Fracture Behavior of Short Circumferentially Surface-Cracked Pipe," NUREG/CR-6298, November 1995.

16 Wilkowski, G. M., Olson, R. J., and Scott, P. M., "State-of-the-Art Report on Piping Fracture Mechanics," U.S.

Nuclear Regulatory Commission report NUREG/CR-6540, BMI-2196, February 1998
17 Graville, B. and Dinovitzer, A., "Strain-Based Failure Criteria for Part-Wall Defects in Pipes," ASME PVP Conference, Montreal, July 1996.
18 DNV Offshore Standard OS-F101, "Submarine Pipeline System," 2000.
19 Kumar, V., German, M. D. and Shih, C. F., "An Engineering Approach for Elastic-Plastic Fracture Analysis," Topical Report No. EPRI NP 1931, Research Project 1237-1, General Electric Co., Schenectady, NY, 1981.
20 Burdekin, F. M. and Dawes, M. G., "Practical Use of Linear Elastic and Yielding Fracture Mechanics with Particular Reference to Pressure Vessels," *Proceedings of the Institute of Mechanical Engineers Conference*, London, May 1971, pp. 28-37.
21 PD 6493:1980, "Guidance on Some Methods for the Derivation of Acceptance Levels for Defects in Fusion Welded Joints," British Standards Institution, March 1980.
22 Wang, Y.-Y., Kirk, M. T., and Reemsnyder, H. "Inference Equations for Fracture Toughness Testing: Numerical Analysis and Experimental Verification," *28th National Symposium on Fatigue and Fracture Mechanics*, ASTM STP 1321, J. Underwood, etc., Eds., Saratoga Springs, NY, June 25-27, 1996.
23 Pick, R. J., Glover, A. G., and Coote, R. I., "Full Scale Testing of Large Diameter Pipelines," Proceedings of Conference on Pipeline and Energy Plant Piping, Pergamon Press, 1980, pp. 357-366.
24 Glover, A. G., Coote, R. I., and Pick, R. J., "Engineering Critical Assessment of Pipeline Girth Welds," Proceedings of Conference on Fitness for Purpose Validation of Welded Construction, The Welding Institute, Paper 30, 1981.
25 Glover, A. G., and Coote, R. I., "Full-Scale Fracture Tests of Pipeline Girth Welds," in Circumferential Cracks in Pressure Vessels and Piping-Vol. II, PVP Vol. 95, G. M. Wilkowski, Eds, 1984, pp. 107-121
26 European Standard, EN 12732, "Gas Supply Systems - Welding Steel Pipework, Functional Requirements," 1999.